

Determination of laser-plasma dispersal velocity and temperature by measuring the lateral-scattering spectrum

V. L. Artsimovich, L. M. Gorbunov, and Yu. S. Kas'yanov

Institute of General Physics, USSR Academy of Sciences
(Submitted 3 June 1985)

Zh. Eksp. Teor. Fiz. **89**, 2026–2032 (December 1985)

The spectrum of lateral (at 90° to the laser-beam axis) scattering with spatial and temporal resolution in a laser plasma produced by second-harmonic emission from a neodymium laser ($\lambda_0 = 0.53 \mu\text{m}$) on a plane target surface is investigated at an energy flux density $< 3 \cdot 10^{14} \text{ W/cm}^2$ and a flux pulse duration $\tau = 2 \text{ ns}$. The results are attributed to Brillouin scattering in the moving plasma, and permit determination of the dependence of the dispersal velocity and of the electron temperature on the distance from the target, as well as an investigation of their variation during the laser pulse.

In experiments on interaction between high-power laser emission and a plasma, much attention is paid to rarefied plasma in which the electron density does not exceed the critical value for the heating-radiation frequency (for the region called plasma corona). The primary reason is that a change of density and temperature in the plasma corona influence strongly the degree of laser-emission scattering, which can reach tens of percent and can lower the target-heating efficiency.

Measurement, with spatial and temporal resolution, of the density, temperature, and dispersal velocity in an inhomogeneous and nonstationary plasma corona is a rather difficult task. Plasma corona is measured at present by optical probing and recording of the heating-radiation harmonics, as well as by x-ray and mass-spectrometer methods.¹ Without dwelling in detail on each of these methods, we note only that they require quite complicated apparatus and the parameters are frequently measured with insufficient spatial and temporal resolution.

Of considerable interest of the diagnostics of laser plasma is investigation of the scattered-radiation spectra near the fundamental frequency. The scattering spectrum was investigated in many experiments mainly in the backward or specular (at oblique incidence on the target) directions. The results lead to definite conclusions concerning the processes that occur in the plasma corona (see, e.g., Refs. 2–4). The spectrum for scattering at large ($\approx 90^\circ$) angles to the laser-beam direction has not been investigated to this day. This is due, on the one hand, to the fact that large-angle scattering by flat targets is negligibly small compared with backscattering or oblique scattering. On the other hand, the apparatus needed to investigate weak lateral scattering must be quite sensitive.

We have investigated in detail, for the first time ever, the spectrum of radiation scattered at 90° to the laser-beam axis. Analysis of the results leads to a new method of determining the dispersal velocity and the electron temperature of a plasma.

The plasma was produced by the second harmonic ($\lambda_0 = 0.53 \mu\text{m}$) of a single-frequency neodymium laser.⁵

The principal parameters of the laser emission were: energy up to 8 J, pulse duration $\approx 2 \text{ ns}$, contrast $> 10^5$, and density of energy flux to the target up to $3 \cdot 10^{14} \text{ W/cm}^2$. The experiments were performed at normal and oblique incidence of *P*-polarized laser emission on flat polyethylene, aluminum, and bismuth targets. The scattering was observed at an angle 90° to the incidence plane of the heating radiation. The experimental setup is shown in Fig. 1a. The scattering region was projected by objective 2 with magnification $\sim 10^\times$ either on the entrance slit of MDR-3 monochromator 5, whose exit plane was coincident with the photocathode plane of electron-optical camera (EDC) 6, or else, directly on the EDC in investigations of the space-time structure of the scattered radiation integrated over the spectrum. Since the intensity of the radiation scattered at 90° was 10^{-7} – 10^{-8} of the heating-radiation intensity, the thermal background was decreased in the latter case by using color filters SZS-22 and ZhS-18. Prism 4 made it possible to vary the orientation of the scattering-region image relative to the monochromator slit. The spatial, temporal, and spectral resolutions were respectively 7 μm , 100 ps, and 1 \AA .

Figure 2a shows a photograph of the scattering over the spectrum, integrated over the time and over the spectrum and obtained for normal incidence of the laser emission on an aluminum target. The size of the scattering region is equal to the size of the laser-beam caustic. (The caustic parameters were measured with a mirror wedge and were: diameter

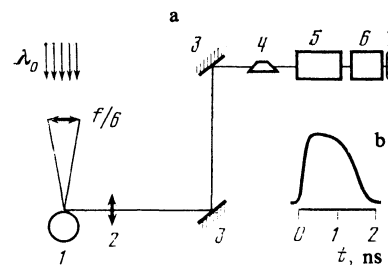


FIG. 1. a) Experimental setup: 1—target, 2—objective, 3—mirrors, 4—turning prism, 5—MDR-3 monochromator, 6—electron-optical camera, 7—photographic film. b) Density pattern of heating pulse.

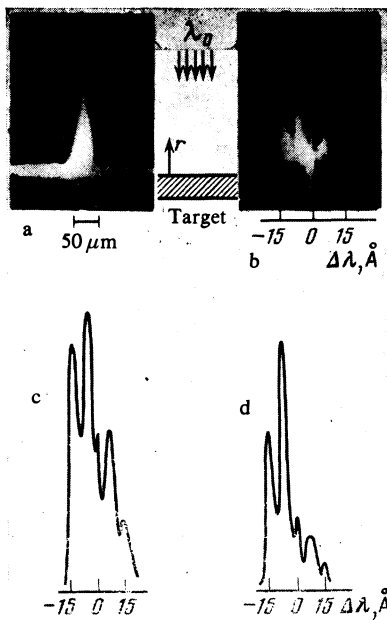


FIG. 2. a) Spatial structure of scattering region (integrated over the spectrum). b) Spatial-spectral structure of scattering region. c) and d) Scattering density patterns at various distances from the target: $r_1 = 50 \mu\text{m}$ (c) and $r_2 = 80 \mu\text{m}$ (d).

$\approx 25 \mu\text{m}$ and length $\approx 1 \text{ mm}$). Time-resolved measurements have shown that the length of the scattering region increases monotonically to a value $\approx 500 \mu\text{m}$ during the time of the heating pulse, contrary to the earlier results of irradiating the targets at wavelength $\lambda = 1.06 \mu\text{m}$, where spatial and temporal pulsations of the scattering region were observed.⁶

The scattered-radiation spectrum consists of two pairs of lines having different intensities and shifted towards longer and shorter wavelengths relative to λ_0 (Fig. 2b). The time-resolved measurement results are shown in Fig. 3. At short distances (less than $50 \mu\text{m}$) from the target scattering was observed during the first nanosecond, apparently because of the increased refraction in the plasma at the later instants of time. It can be seen from Fig. 3a that the spectral lines are broadened and their shift from λ_0 increases with time. As the distance from the target is increased (Figs. 3b, c) the intensity of the "red" satellites decreases substantially, the instant at which the scattering appears is delayed, while both "blue" satellites appear simultaneously.

To ascertain the cause of the four-component structure of the spectrum, experiments were performed with oblique incidence of the laser emission on the target. The image of the target surface was oriented in this case parallel to the monochromator slit. In this experimental geometry, the satellites were observed to shift along the target surface T (the x coordinate, Fig. 4.). At a given incidence angle, the shift is larger the farther the target-surface image from the monochromator slit. This has shown that in oblique incidence the short-wave (blue) and long-wave (red) satellites are due respectively to scattering of the laser emission incident on the plasma and specularly reflected from the critical plane. At sufficient degree (several percent) of backscattering into the

focusing lens one more satellite pair appears in the back-scattering radiation and is due to Stokes component of stimulated Brillouin scattering. We note that in all experiments the scattering-radiation polarization was close to linear and coincided with the incident-radiation polarization.

The observed linear growth of the intensity of the blue satellites with increasing laser-emission flux density indicates that this scattering is not stimulated. This conclusion is confirmed also by the fact that the total reflection coefficient of the incident radiation differs little from the intensity ratio of the red and blue lines.

To estimate the fraction E of the scattered energy we use the relation⁷

$$\Delta E \sim N_e r_0^2 L E \Delta \Omega, \quad (1)$$

where N_e is the electron density, $r_0 = e^2/mc^2 = 2.8 \cdot 10^{-13} \text{ cm}$ is the electron classical radius, L is the length of the scattering volume, E is the incident radiation, and $\Delta \Omega$ is the solid angle of the receiving apparatus. Substituting values typical of our experiment, $\Delta \Omega \approx 8 \cdot 10^{-2} \text{ sr}$, $L \approx 300 \mu\text{m}$, and $N_e \approx 10^{20} \text{ cm}^{-3}$, we find that $\Delta E/E \approx 2 \cdot 10^{-8}$ for scattering by thermal fluctuations. This value agrees satisfactorily with the scattered-energy estimates obtained by experiment.

The linear dependence of the scattering intensity on N_e allows us to estimate the change of the correlation along the caustic of the heating radiation (Fig. 5). The estimate was obtained with allowance for the dependence of the scattering duration on the distance to the target. For $N_e \approx 10^{20} \text{ cm}^{-3}$ at a distance $\approx 100 \mu\text{m}$ from the target we used an estimate previously obtained by the Schlieren method.⁸

The foregoing results of the spectral measurements, and also the scattering-energy level, can be interpreted as lateral Brillouin scattering in a supersonic plasma. In this case the spectral shifts of the blue satellites are determined by the frequencies of the sound waves in the moving plasma, and their values at normal incidence are

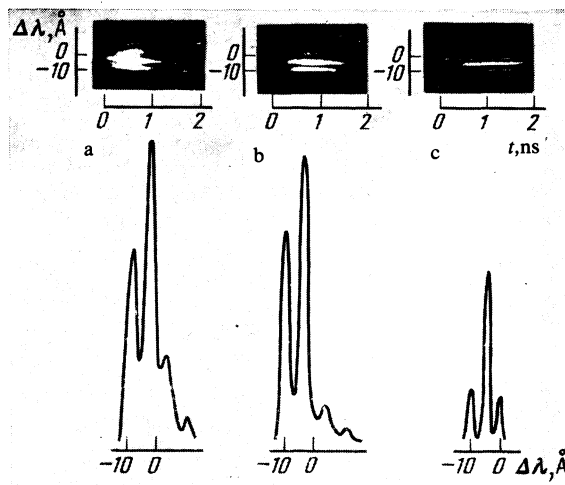


FIG. 3. Temporal spectrograms of the scattering at various distances from the target, and density patterns of the spectra at various instant of time: a— $r_1 = 45 \mu\text{m}$, $t = 0.5 \text{ ns}$; b— $r_2 = 90 \mu\text{m}$, $t = 1 \text{ ns}$; c— $r_3 = 180 \mu\text{m}$, $t = 1.5 \text{ ns}$.

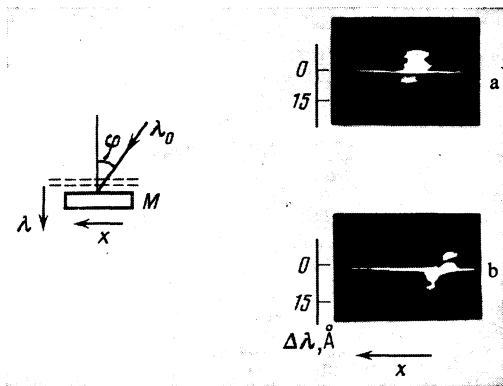


FIG. 4. Experiments with oblique incidence: observation geometry (left) and scattering spectrograms for incidence angles $\varphi = 20^\circ$ (a) and $\varphi = 45^\circ$ (b).

$$\Delta\lambda_{1,2}^b = \lambda_0 - \lambda_{1,2}^b = \frac{\lambda_0}{c} \left(1 - \frac{N_e}{N_c}\right)^{1/2} \left[V \mp \frac{2^{1/2} V_s}{(1 + 2k_0^2 a_e^2)^{1/2}} \right], \quad (2)$$

where $\lambda_{1,2}^b$ is the wavelength of the blue satellites, λ_0 and k_0 are the wavelength and wave vector of the laser radiation, V is the plasma dispersal velocity, $V_s = (zT_e/m_i)^{1/2}$ is the speed of sound in the plasma, a_e is the electron Debye radius, $(1 - N_e/N_c)^{1/2}$ is the refractive index and is close to unity in the rarefied corona ($N_e/N_c \ll 1$) in which the scattering is observed, and N_c is the critical density.

Expressing V and V_s from (2) in terms of the experimentally measured parameters $\Delta\lambda_{1,2}^b$, we obtain

$$V = (c/2\lambda_0) (\Delta\lambda_1^b + \Delta\lambda_2^b), \quad (3)$$

$$V_s (1 + 2k_0^2 a_e^2)^{-1/2} = (c/2^{1/2}\lambda_0) (\Delta\lambda_2^b - \Delta\lambda_1^b). \quad (4)$$

It is easy to determine, with the aid of (3), the plasma-dispersal velocity at various distances from the target. The reduced experimental data are shown in Fig. 5.

Equation (4) leads to an expression for the electron temperature:

$$T_e = \frac{m_i c^2}{z} \frac{(\Delta\lambda_2^b - \Delta\lambda_1^b)^2}{8\lambda_0^2} \left[1 - \frac{m_i}{z m_e} \frac{N_c}{N_e} \frac{(\Delta\lambda_2^b - \Delta\lambda_1^b)^2}{4\lambda_0^2} \right]^{-1}, \quad (5)$$

where m_i is the ion mass. Since $(\Delta\lambda_2^b - \Delta\lambda_1^b)/\lambda_0 \sim 10^{-3}$, the second term in the square bracket is negligibly small at $N_e < 10^{-2} N_c$ or at a distance of more than $150 \mu\text{m}$ from the target (see Fig. 5). This enables us to simplify Eq. (5):

$$T_e \approx \frac{m_i c^2}{z} \frac{(\Delta\lambda_2^b - \Delta\lambda_1^b)^2}{8\lambda_0^2}. \quad (6)$$

A form more suitable for calculations is

$$T_e \approx 4.2 (A/z) (\Delta\lambda_2^b - \Delta\lambda_1^b)^2, \quad (7)$$

where A is the atomic number of the target material, $\Delta\lambda$ is in angstroms, and T_e is in electron volts. Formula (7) for short distances from the target was used to calculate the electron temperatures T_e for polyethylene, aluminum, and bismuth targets; the values were 500, 600, and 1000 eV, respectively.

It should be noted that at a considerable distance from the target surface ($r > 150 \mu\text{m}$) the value of $\Delta\lambda_2^b - \Delta\lambda_1^b$ decreases (Fig. 2b) in such a way that even though N_e/N_c

increases. The value of T_e calculated from (5) remains practically constant at the value of T_e at short distances from the target. This points to isotropic dispersal of the laser plasma in our experiments.

The red-satellite displacement due to Brillouin scattering of the radiation reflected from the plasma is given by an expression similar to (2):

$$\Delta\lambda_{1,2}^r = \lambda_0 - \lambda_{1,2}^r = -\frac{\lambda_0}{c} [V \mp 2^{1/2} V_s] + \Delta\lambda_{\text{sh}}; \quad (8)$$

here $\lambda_{1,2}^r$ are the wavelengths of the red satellites, and $\Delta\lambda_{\text{sh}}$ is the laser-wavelength shift upon reflection from the dense layers of the plasma. The factor $(1 + 2k_0^2 a_e^2)^{-1/2}$ has been omitted, since intense scattering in the long-wave region of the spectrum is observed near the target (Fig. 2). From (2) and (8) it follows that

$$\Delta\lambda_{\text{sh}} = |\Delta\lambda_1^r| - \Delta\lambda_1^b = |\Delta\lambda_2^r| - \Delta\lambda_2^b. \quad (9)$$

The shift $\Delta\lambda_{\text{sh}}$ can be due, generally speaking, to two factors: specular reflection of the laser emission from the moving critical density (Doppler effect), or stimulated Brillouin backscattering. At oblique incidence (in experiments performed only with aluminum targets) one can separate the specular component (see Fig. 4). In this case the velocity of the critical density is given by

$$V_c = \Delta\lambda_{\text{sh}} c / 2\lambda_0 \cos \varphi, \quad (10)$$

where φ is the angle of incidence angle of the laser radiation on the target.

At an incidence angle $\varphi = 20^\circ$ and a flux density $q \approx 10^{14} \text{ W/cm}^2$ the velocity is $V_c \approx 4 \cdot 10^6 \text{ cm/s}$ and is directed inward into the target. The reason why the critical density moves into the target interior at this velocity (this is precisely when sufficiently intense scattering of the long-wave satellites is observed, see Fig. 3a) remains unclear.

We note that in accordance with the organization of the experiments, the laser-plasma parameters T_e , V , and V_c , which we calculated from the scattering-line shifts, were averaged over the plasma volume determined by the diameter of the heating-radiation caustic ($20\text{--}25 \mu\text{m}$) and by the spatial resolution of the recording system ($\approx 7 \mu\text{m}$).

The difference between the Stokes- and anti-Stokes component intensities (Figs. 2c, d) indicates that the sound-wave spectrum in the plasma is anisotropic. This anisotropy can be due to generation and emission of sound waves from

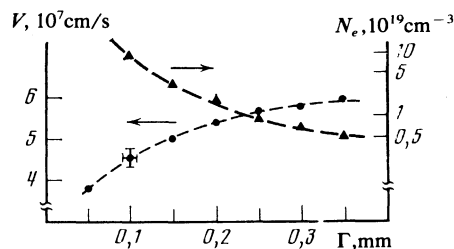


FIG. 5. Plasma-dispersal velocity, determined by measuring the scattering spectrum, vs distance to the target surface. N_e is the plasma-electron density estimated from the scattered-radiation intensity.

the dense plasma layer, or to the flow of spontaneous-magnetic-field generating currents in the plasma.⁸ It is possible that the high intensity of the Stokes line is connected with the stimulated-scattering process. Estimates show that under the conditions of these experiments the gain of the lateral Brillouin scattering is close to unity.

In conclusion, we compare our results with those obtained by other methods. The asymptotic expansion velocity $V_{as} = (4-6) \cdot 10^7$ cm/s, measured by scanning the plasma intrinsic radiation,⁹ agrees fairly well with our data. The electron temperature T_e was measured by two methods. The value obtained in the corona at $1.06 \mu\text{m}$ wavelength and at the corresponding flux density by the method of x-ray absorbers was $T_e = 400-500$ eV for a carbon target.¹⁰ It follows from the results of Refs. 11 and 12 that, other conditions being equal, the corona temperature depends very little on the wavelength of the heating radiation, namely, $T_e \propto \lambda^{0.3}$. It can therefore be assumed that at $0.53 \mu\text{m}$ wavelength the electron temperature is also close to this value. A method based on analyzing the spectrum near a frequency $(3/2)\omega_0$ (Ref. 5) yields approximately double the value of T_e obtained by us. That the method of half-interger harmonics yields higher values of T_e than the absorber method has been reported earlier.¹³ This discrepancy can be due, on the one hand, to local overheating of the corona close to one-quarter the critical density, and on the other to the limitations of the theoretical models used to calculate the spectra.

It can thus be concluded that the proposed method of determining laser-plasma parameters by measuring the spectrum of lateral Brillouin scattering agrees well with results of measurements by other methods and permits measure-

ments, with high temporal and spatial resolution, of the dispersal velocity and temperature of the electrons in a laser-plasma corona.

- ¹N. G. Basov, Yu. A. Zakharenkov, N. N. Zorev, *et al.*, *Itogi Nauki i Tekhniki, Radiofizika* (Science and Engineering Summaries, Radiophysics), VINITI, 1982, 26.
- ²M. D. Rosen, D. W. Phillion, V. C. Rupert, *et al.*, *Phys. Fluids* **22**, 2020 (1979).
- ³O. G. Baïkov, V. I. Bayanov, A. A. Mak, *et al.*, *Pis'ma Zh. Eksp. Teor. Fiz.* **29**, 44 (1979) [*JETP Lett.* **29**, 40 (1979)].
- ⁴V. L. Artsimovich, L. M. Gorbunov, Yu. S. Kas'yanov, and V. V. Korobkin, *Zh. Eksp. Teor. Fiz.* **80**, 1859 (1981) [*Sov. Phys. JETP* **53**, 963 (1981)].
- ⁵V. Yu. Bychenkov, A. A. Zozulya, Yu. S. Kas'yanov, *et al.*, *ibid.* **84**, 936 (1983) [*Sov. Phys. JETP* **57**, 544 (1983)].
- ⁶V. L. Artsimovich, L. M. Gorbunov, Yu. S. Kas'yanov, and V. V. Korobkin, *Dokl. Akad. Nauk SSSR* **265**, 857 (1982) [*Sov. Phys. Dokl.* **27**, 618 (1982)].
- ⁷J. Sheffield, *Scattering of Electromagnetic Radiation in a Plasma* [Russ. transl.] Atomizdat, 1978, p. 48.
- ⁸F. V. Bunkin, Yu. S. Kas'yanov, V. V. Korobkin, and S. L. Motylev, *Kvant. Elektron.* (Moscow) **10**, 2149 (1983) [*Sov. J. Quant. Electron.* **13**, 1437 (1983)].
- ⁹P. Y. Pirogovskii and A. P. Shevel'ko, FIAN Preprint No. 82, 1984.
- ¹⁰Y. S. Kas'yanov, V. K. Chevokin, A. P. Shevel'ko, and M. Ya. Shchelev, *Pis'ma Zh. Tekh. Fiz.* **3**, 1156 (1977) [*Sov. J. Tech Phys. Lett.* **3**, 476 (1977)].
- ¹¹W. C. Mead, E. M. Campbell, K. G. Estabrook, *et al.*, *Phys. Fluids* **26**, 2316 (1983).
- ¹²H. Nishimura, H. Azechi, K. Yamada, *et al.*, *Phys. Rev.* **A23**, 2011 (1981).
- ¹³L. M. Gorbunov, Yu. S. Kas'yanov, V. V. Korobkin, *et al.*, FIAN Preprint No. 126, 1979.

Translated by J. G. Adashko